Biophysical Chemistry 155 (2011) 65–73

Contents lists available at ScienceDirect

Biophysical Chemistry

journal homepage: http://www.elsevier.com/locate/biophyschem

Nutrient diffusion and simple n[th]-order consumption in regenerative tissue and biocatalytic sensors ☆

Laurence A. Belfiore *, Michael L. Floren [1], Fabio Z. Volpato [1], Alexandre T. Paulino, Carol J. Belfiore

Department of Chemical & Biological Engineering, Colorado State University, Fort Collins, Colorado, 80523, USA

ARTICLE INFO

Article history:
Received 31 December 2010
Received in revised form 17 February 2011
Accepted 17 February 2011
Available online 23 February 2011

Keywords:
Fick's second law
Unsteady state diffusion
Modified diffusion equation
Reaction–diffusion equation
Zeroth-order reaction
Intra-tissue Damköhler number
Critical Damköhler number
Regenerative tissue
Biosensors
von Kármán–Pohlhausen profile method
Mass transfer boundary layer thickness

ABSTRACT

This contribution addresses intra-tissue molar density profiles for nutrients, oxygen, growth factors, and other essential ingredients that anchorage-dependent cells require for successful proliferation on biocompatible surfaces. One-dimensional transient and steady state models of the reaction–diffusion equation are solved to correct a few deficiencies in the first illustrative example of diffusion and zeroth-order rates of consumption in tissues with rectangular geometry, as discussed in Ref. [(Griffith and Swartz, 2006) 1]. The functional form of the molar density profile for each species depends on geometry and the magnitude of the species-specific intra-tissue Damköhler number. The tissue's central core is reactant starved at high consumption rates and low rates of intra-tissue diffusion when the Damköhler number exceeds its geometry-sensitive critical value. Ideal tissue engineering designs avoid the diffusion-limited regime such that attached cells are exposed to all of the ingredients required for proliferation everywhere within a regenerative matrix. Analytical and numerical molar density profiles that satisfy the unsteady state modified diffusion equation with pseudo-homogeneous n[th]-order rates of intra-tissue consumption (i.e., n = 0,1,2) allow one to (i) predict von Kármán–Pohlhausen mass transfer boundary layer thicknesses, measured inward from the external biomaterial surface toward its central core, and, most importantly, (ii) estimate the time required to achieve steady state conditions for regenerative tissue growth and biocatalytic sensing.

1. Dimensionless mass balance for steady state one-dimensional diffusion and zeroth-order consumption in regenerative tissue and biocatalytic sensors with rectangular symmetry

Steady state and transient response of biocatalytic sensors can be modeled by analyzing diffusion and chemical reaction in mammalian tissue with anchorage-dependent cells [2,3]. Under steady state conditions, homogeneous one-dimensional diffusion, accompanied by zeroth-order rates of chemical reaction in rectangular geometries for nutrients, oxygen, or growth factors such as EGF (i.e., reactant A), is described by the following dimensionless mass balance (i.e., the reaction–diffusion equation) [4];

$$\nabla^2\Psi_A \overset{1-\text{dimensional}}{\underset{\text{diffusion}}{\Rightarrow}} \frac{d^2\Psi_A}{d\eta^2} = \Lambda_A^2 R^* = \Lambda_A^2 \tag{1}$$

where $\eta = x/L$, with a tissue thickness of 2L in its thinnest dimension, $\eta = 0$ along the centerline of the tissue, $\Psi_A = C_A/C_{A,Surface}$, and Λ_A^2 is the species-specific intra-tissue Damköhler number that represents an order-of-magnitude ratio of the consumption rate to the rate of diffusion toward anchorage-dependent cells [4]. Hence:

$$\Lambda_A^2 = \frac{k_{Rx,n} L^2 C_{A,Surface}^{n-1}}{D_{A,effective\ \text{intra}-tissue}} \tag{2}$$

where $C_{A,Surface}$ is the molar density of species *A* on the external tissue surface, $k_{Rx,n}$ is the pseudo-volumetric kinetic rate constant for n[th]-order consumption, and $D_{A,effective\ \text{intra-}tissue}$ is the effective diffusion coefficient for species *A* that accounts for the porous and tortuous nature of a biomaterial matrix. The Damköhler number (i.e., a reaction–diffusion parameter) has been employed previously to model reaction and diffusion in cell cultures [5,6], micro-channel bioreactors [7], and electrochemical biosensors immobilized within a highly dispersed mesh of carbon nanotubes [8]. The *pressure-sensitive* Damköhler number was developed recently to quantify mechano-sensitive zeroth-order bone tissue growth in response to centrifugal-force-induced hydrostatic pressure modulations in rotating-cup bioreactors [9]. The concept of the intra-tissue Damköhler number is analogous to the intrapellet Damköhler number for heterogeneous catalysis in packed reactors [4,10]. Under isothermal conditions,

☆ This manuscript commemorates the 100th anniversary of the birth of Olivia DeVito Belfiore on June 18th, 1911, and the death of her mother upon childbirth. It is submitted in memory of my best childhood friend, Frank Daniel DeVito, whose 56th birthday would have occurred on Dec. 6th, 2010.

* Corresponding author, presently at: Department of Materials Engineering & Industrial Technologies, University of Trento, via Mesiano 77, 38050 Trento, Italy.
E-mail address: belfiore@engr.colostate.edu (L.A. Belfiore).
[1] Presently at: Department of Materials Engineering & Industrial Technologies, University of Trento, via Mesiano 77, 38050 Trento, Italy.

0301-4622/$ – see front matter © 2011 Elsevier B.V. All rights reserved.
doi:10.1016/j.bpc.2011.02.005

kinetic rate constants in the bulk tissue are the same as those on the external surface, and the dimensionless rate law R^* in the dimensionless mass balance is [4];

$$R^* = \frac{k_{Rx,n}(T)C_A^n}{k_{Rx,n}\left(T_{Surface}\right)C_{A,Surface}^n} = \Psi_A^n \underset{zeroth-order\ kinetics}{\overset{n=0}{\Rightarrow}} 1 \tag{3}$$

The second-order ordinary differential equation, which represents the mass balance for one-dimensional diffusion and zeroth-order consumption, is very simple to integrate. The molar density profile for nutrients, oxygen, and growth factors is a quadratic function of spatial coordinate η, measured from the centerline in the thinnest dimension of the tissue. These composition profiles are given by slightly distorted quadratic functions in regenerative tissue and biosensing devices with cylindrical and spherical symmetry. Conceptual difficulty arises for zeroth-order kinetics because it is necessary to introduce a critical dimensionless spatial coordinate, $\eta_{critical}$, which has the following physically realistic definition.

When $\eta_{critical}$, which is a function of the intra-tissue Damköhler number, adopts values between 0 and 1, then regions within the central core of the tissue are inaccessible to the reactants (i.e., nutrients, oxygen, and growth factors) because the consumption rate is much faster than the rate of species-specific diffusion. The thickness of the dimensionless mass transfer boundary layer for each of the reactants, measured inward from the external surface of the tissue, is $1-\eta_{critical}$.

The quantitative definition of this critical spatial coordinate is;

$$\Psi_A(\eta = \eta_{critical}) = 0 \tag{4}$$

Two constants of integration appear when the mass balance is solved for the basic information, $\Psi_A = f(\eta)$. These two integration constants together with $\eta_{critical}$ represent three unknowns that are determined from two boundary conditions and the mathematical definition of the critical spatial coordinate. Hence, the three conditions are;

$$\begin{aligned}
&(i) \quad \Psi_A(\eta = 1) = 1, \textit{ on the external tissue surface}\\
&(ii,a) \left\{\frac{d\Psi_A}{d\eta}\right\}_{\eta=\eta_{critical}} = 0, \textit{ when } \Lambda_A > \Lambda_{A,critical}\\
&(ii,b) \left\{\frac{d\Psi_A}{d\eta}\right\}_{\eta=0} = 0, \textit{ when } \Lambda_A \le \Lambda_{A,critical}\\
&(iii) \quad \Psi_A(\eta = \eta_{critical}) = 0
\end{aligned} \tag{5}$$

$\eta_{critical}$ is required for diffusion and zeroth-order reaction under transient and steady state conditions. If reactants achieve zero molar density with zero flux at $\eta_{critical}$, then there is no driving force for them to diffuse further inward. Hence, conditions (ii-a) and (iii) are reasonable. When $\eta_{critical}<0$, condition (ii-b) must be employed, which is consistent with the well-known symmetry condition in the tissue's central core when rates of consumption depend on reactant molar density [5]. If one invokes zero flux at the symmetry plane (i.e., $x=0$ or $\eta=0$) when the Damköhler number is too large, then the mass balance with diffusion and zeroth-order reaction will predict negative reactant molar density in the central core. Under steady state conditions, zero flux at the symmetry plane is correct for all kinetic rate laws, except zeroth-order kinetics when the Damköhler number exceeds its critical value and the tissue's central core is reactant starved. Zeroth-order rates of reaction that do not depend on molar densities must be extinguished in the central core when reactants are depleted completely. Whereas zeroth-order kinetics might represent a reasonable model over a wide range of reactant molar densities, this simple model is atrociously incorrect when reactants are consumed completely, or diffusion is hindered such that reactants do not penetrate the intra-tissue core. Hence, the mass balance for pseudo-homogeneous one-dimensional diffusion and zeroth-order consumption is solved only over the following range of the independent variable; $\eta_{critical} \le \eta \le 1$, when $\eta_{critical}$ is between 0 and 1. The critical spatial coordinate $\eta_{critical}$ is negative when the intra-tissue Damköhler number is smaller than its critical value. Under these conditions, the mass balance is solved over the complete range of η (i.e., between 0 and 1) when $\Lambda_A<\Lambda_{A,critical}$ and boundary condition (ii-b) is employed. The critical value of the intra-tissue Damköhler number is defined mathematically as;

$$\eta_{critical}\left(\Lambda_A = \Lambda_{A,critical}\right) = 0 \tag{6}$$

Hence, reactants exist everywhere within the tissue when the consumption rate is slow enough relative to species-specific diffusion, and the intra-tissue Damköhler number is less than, or equal to, its critical value. These conditions yield an effectiveness factor E of unity for zeroth-order consumption [4], where E is equivalent to the volume fraction of the biomaterial that contains the required ingredients for cell proliferation. When the intra-tissue Damköhler number is greater than $\Lambda_{A,critical}$, the central core of the tissue is reactant starved because $\eta_{critical}$ is between 0 and 1, and the effectiveness factor decreases below unity because reactant consumption occurs only in the outer regions of the tissue, near its external surface. Dimensionless correlations between the effectiveness factor and the tissue-based Damköhler number [4,5] for zeroth-order rates of consumption exhibit an abrupt decrease in slope (i.e., from 0 to −1 on log-log coordinates) when $\Lambda_A = \Lambda_{A,critical}$. If one does not impose zero reactant molar density and zero flux at $\eta_{critical}$ for zeroth-order kinetics, then steady state effectiveness factor correlations intersect those for other simple n^{th}-order rate laws in systems with the same geometry, instead of defining the asymptotes at large and small Damköhler numbers. Critical spatial coordinates and critical intra-tissue Damköhler numbers are not required to analyze homogeneous steady state diffusion and chemical reaction in biological materials when the consumption rate is not zeroth-order, because simple n^{th}-order rates of consumption become vanishingly small when reactant molar densities decrease to a negligible fraction of their values on the external tissue surface. However, boundary conditions at $\eta_{critical}$ given by Eq. (5) are employed to analyze time-dependent inward growth of the mass transfer boundary layer thickness δ_{MTBLT} via the von Kármán–Pohlhausen integral analysis of the modified diffusion equation for all types of biomaterial geometries and consumption rates, where $\delta_{MTBLT} = 1-\eta_{critical}$.

2. Critical dimensionless spatial coordinate and intra-tissue Damköhler number for steady state diffusion and zeroth-order consumption in rectangular geometries

When the differential mass balance for 1-dimensional diffusion and zeroth-order kinetics;

$$\frac{d^2\Psi_A}{d\eta^2} = \Lambda_A^2 \tag{7}$$

is integrated twice, subject to the following boundary conditions;

$$\begin{aligned}
&(i) \quad \Psi_A(\eta = 1) = 1\\
&(ii,a) \left\{\frac{d\Psi_A}{d\eta}\right\}_{\eta=\eta_{critical}} = 0
\end{aligned} \tag{8}$$

the following quadratic function is obtained;

$$\Psi_A(\eta; \eta_{critical}, \Lambda_A) = 1 + \Lambda_A^2\eta_{critical}(1-\eta) - \frac{1}{2}\Lambda_A^2\left(1-\eta^2\right) \tag{9}$$

This is the basic information governed by the mass balance, from which the dimensionless correlation between the effectiveness factor and the tissue-based Damköhler number is generated. When;

$$\Psi_A(\eta = \eta_{critical}; \eta_{critical}, \Lambda_A) = 0 \tag{10}$$

is implemented to define the critical dimensionless spatial coordinate, the resulting quadratic equation can be solved analytically for $\eta_{critical}$. The following expression is obtained;

$$\eta_{critical}(\Lambda_A) = 1 - \frac{\sqrt{2}}{\Lambda_A} \tag{11}$$

where the smaller of the two solutions is chosen to ensure that $\eta_{critical} < 1$. In agreement with physical reality, $\eta_{critical}$ increases at higher values of the intra-tissue Damköhler number, which implies that a larger fraction of the tissue's core is reactant starved at higher consumption rates, and the mass transfer boundary layer thickness occupies a thinner region near the external biomaterial surface. The critical dimensionless spatial coordinate is zero (i.e., $\eta_{critical} = 0$) when the intra-tissue Damköhler number achieves its critical value;

$$\Lambda_{A,critical} = \sqrt{2} \tag{12}$$

for zeroth-order rates of consumption in tissue with rectangular geometry. Steady state molar density profiles based on Eqs. (9) and (11) are illustrated in Fig. 1 for intra-tissue Damköhler numbers that are above and below $\Lambda_{A,critical}$. When the intra-tissue Damköhler number is less than its critical value, the critical dimensionless spatial coordinate $\eta_{critical}$ is negative, and boundary condition (ii-b) must be employed instead of (ii-a). Under these conditions, the dimensionless intra-tissue molar density profile for reactant A is adopted from Eq. (9) by setting $\eta_{critical}$ to zero. Hence;

$$\Psi_A(\eta; \Lambda_A) \overset{\substack{\Lambda_A \le \Lambda_{A,critical} \\ \Rightarrow \\ \eta_{critical} = 0}}{} 1 - \frac{1}{2}\Lambda_A^2\left(1 - \eta^2\right) \tag{13}$$

In this *non-diffusion-limited regime,* steady state reactant molar densities do not decrease to zero along the centerline of the tissue, where $\eta = 0$, when the intra-tissue Damköhler number is below its critical value;

$$\Psi_A\left(\eta = 0; \Lambda_A < \sqrt{2}\right) = 1 - \frac{1}{2}\Lambda_A^2 > 0 \tag{14}$$

Hence, the required ingredients for cell proliferation and biocatalytic sensing exist throughout the biomaterial at steady state, and Ψ_A decreases when Λ_A is larger.

3. Steady state differential mass balances, molar density profiles, and the functional dependence of $\eta_{critical}$ on Λ_A for zeroth-order consumption in biomaterials with cylindrical and spherical symmetry

The pseudo-homogeneous one-dimensional diffusion model is slightly more complex in cylindrical and spherical coordinates, relative to the model described above in rectangular coordinates. Additional complexity arises because the radial contribution to the Laplacian operator ($\nabla\bullet\nabla = \nabla^2$) accounts for the fact that the surface area across which radial diffusion occurs increases linearly with dimensionless radial coordinate $\eta = r/R$ as one moves radially outward from the central axis of a cylinder [4,10]. For spheres, surface area scales as η^2 as one moves radially outward from the central point. Reactant molar density profiles are obtained by integrating the dimensionless mass balance with radial diffusion and zeroth-order rates of consumption [4];

$$\frac{1}{\eta^\alpha}\frac{d}{d\eta}\left\{\eta^\alpha \frac{d\Psi_A}{d\eta}\right\} = \Lambda_A^2 \tag{15}$$

subject to two boundary conditions and the definition of $\eta_{critical}$, described above. The *curvature correction exponent* α is 1 for cylinders and 2 for spheres [4,5]. Distorted quadratic functions are obtained for reactant molar density in curvilinear coordinates;

$$\begin{aligned} &Cylinders: \Psi_A(\eta; \eta_{critical}, \Lambda_A) = 1 - \frac{1}{4}\Lambda_A^2\left(1 - \eta^2\right) - \frac{1}{2}\left\{\Lambda_A \eta_{critical}\right\}^2 \ln\eta \\ &Spheres: \Psi_A(\eta; \eta_{critical}, \Lambda_A) = 1 - \frac{1}{6}\Lambda_A^2\left(1 - \eta^2\right) - \frac{1}{3}\Lambda_A^2 \eta_{critical}^3\left\{1 - \eta^{-1}\right\} \end{aligned} \tag{16}$$

Critical dimensionless spatial coordinates $\eta_{critical}$ are calculated by solving the previous two nonlinear algebraic equations for roots between $0 \le \eta = \eta_{critical} \le 1$ where species molar density vanishes in the tissue's central core when the intra-tissue Damköhler number exceeds its critical value. Dependence of $\eta_{critical}$ on Λ_A is summarized in Table 1 for cylinders and spheres. Numerical results for $\eta_{critical}$ vs. Λ_A are geometry-insensitive when $\Lambda_A \ge 15$. In this regime of intra-tissue Damköhler numbers, the analytical expression given by Eq. (11), $\eta_{critical} = f(\Lambda_A) = 1 - \sqrt{(2)}/\Lambda_A$, for biomaterials with rectangular symmetry can be used to predict dimensionless intra-tissue spatial

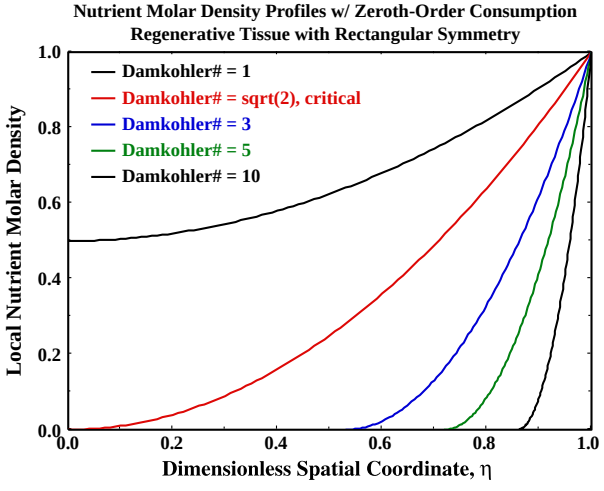

Fig. 1. Effect of the species-specific intra-tissue Damköhler number Λ_A on dimensionless molar density profiles for nutrients, oxygen, and growth factors in mammalian tissue and biocatalytic sensors with rectangular symmetry. The steady state model includes one-dimensional diffusion and pseudo-homogeneous zeroth-order consumption. Molar density profiles are illustrated at sub-critical (i.e., $\Lambda_A = 1$), critical (i.e., $\Lambda_A = \sqrt{2}$), and super-critical (i.e., $\Lambda_A = 3,5,10$) Damköhler numbers. The intra-tissue Damköhler number increases from the uppermost curve to the lowermost curve.

Table 1
Effect of the intra-tissue Damköhler number on the critical dimensionless radius for radial diffusion and pseudo-homogeneous zeroth-order consumption in biomaterials with cylindrical and spherical symmetry. The characteristic length L in the definition of Λ_A is the cylindrical or spherical radius R.

Λ_A	$\eta_{critical,cylinder}$	$\eta_{critical,sphere}$	Λ_A	$\eta_{critical,cylinder}$	$\eta_{critical,sphere}$
2.0	0	–	6.0	0.75	0.74
√(6)	0.32	0	6.5	0.77	0.76
3.0	0.47	0.39	7.0	0.79	0.78
3.5	0.56	0.51	7.5	0.80	0.79
4.0	0.62	0.58	8.0	0.82	0.81
4.5	0.66	0.64	9.0	0.84	0.83
5.0	0.70	0.68	10	0.86	0.85
5.5	0.73	0.71	15	0.90	0.90

distances measured from the external surface (i.e., $1-\eta_{critical}$), where reactants vanish, regardless of macroscopic shape. For all biomaterial geometries, $\eta_{critical} \Rightarrow 1$ in the diffusion-limited regime when $\Lambda_A \Rightarrow \infty$, such that the mass transfer boundary layer thickness measured inward from the external tissue surface is infinitesimally small.

In the *non-diffusion-limited regime,* when intra-tissue Damköhlers numbers do not exceed their geometry-sensitive critical values and the required ingredients for cell proliferation and sensing exist throughout the biomaterial, steady state reactant molar densities in the central core of the tissue at $\eta=0$ can be predicted as follows;

$$\begin{aligned} &\textit{Cylinders}: \Psi_A(\eta=0;\Lambda_A<2) = 1-\frac{1}{4}\Lambda_A^2 > 0 \\ &\textit{Spheres}: \Psi_A\left(\eta=0;\Lambda_A<\sqrt{6}\right) = 1-\frac{1}{6}\Lambda_A^2 > 0 \end{aligned} \tag{17}$$

4. Critical intra-tissue Damköhler numbers for simple geometries

Critical values of the intra-tissue Damköhler number are summarized below for three simple biomaterial geometries;

(i) $\Lambda^2_{A,critical}=2$, for tissue with rectangular symmetry
(ii) $\Lambda^2_{A,critical}=4$, for long cylinders, and
(iii) $\Lambda^2_{A,critical}=6$, for spheres,

when the corresponding characteristic length L in the Damköhler number is defined as;

(i) one-half of the tissue thickness, measured in the thinnest dimension
(ii) the radius of long cylinders
(iii) the radius of a sphere

One common characteristic of these length scales is that the dimensionless spatial coordinate is identically zero at the intra-tissue plane, axis, or point of symmetry, and η reaches its maximum value of unity on the external tissue surface. In light of universal correlations, a typical characteristic length scale for all tissue shapes might be postulated as follows [10];

$$L = \frac{V_{tissue}}{S_{external}} \tag{18}$$

where V_{tissue} is the tissue volume, and $S_{external}$ is its total external surface area, excluding the edges of rectangular biomaterial and the circular ends of cylinders. This definition of L reduces to;

(i) one-half of the thickness of rectangular tissue, measured in the thinnest dimension
(ii) one-half of the radius of long cylinders, and
(iii) one-third of the radius of a sphere.

These characteristic lengths L yield the following critical values of the intra-tissue Damköhler number for biomaterials that exhibit macroscopic symmetry in rectangular, cylindrical, or spherical coordinates;

(i) $\Lambda^2_{A,critical}=2$ for tissue with rectangular symmetry
(ii) $\Lambda^2_{A,critical}=1$ for long cylinders
(iii) $\Lambda^2_{A,critical}=0.67$ for spheres

Curvature is not important at large intra-tissue Damköhler numbers, when nutrients, oxygen, and growth factors exist only in a thin shell near $\eta=1$ and, consequently, a locally flat description of the problem is appropriate for any geometry. These comments apply equally well to other types of kinetic rate laws that describe reactant consumption.

5. Transient description of one-dimensional diffusion and nth-order consumption in biomaterials with rectangular symmetry

Fick's second law of diffusion with nth-order consumption (i.e., the *modified diffusion equation*) describes the transient and spatial dependence of the molar density of each reactive species (i.e., nutrients, oxygen, growth factors, etc.) within a biocatalytic sensor [2,3] or regenerative matrix of thickness 2L. For one-directional flux in the x-direction across the thinnest dimension of this matrix, one must solve the following equation for $C_A(t,x)$;

$$\frac{\partial C_A}{\partial t} = D_{A,effective\ \mathrm{intra-tissue}}\frac{\partial^2 C_A}{\partial x^2} - k_{Rx,n}C_A^n \tag{19}$$

where time t accounts for transient response, $k_{Rx,n}$ is a pseudo-homogeneous nth-order kinetic rate constant for reactant consumption by anchorage-dependent cells within the matrix, and all other variables have been defined previously. Both sides of the regenerative matrix (i.e., $x=\pm L$) are exposed to a well-mixed nutrient medium at time, $t=0$. The required boundary conditions for zeroth-order nutrient consumption (i.e., $n=0$) are;

$$\begin{aligned} &C_A = C_{A,medium} \quad x = L;\ t>0 \\ &\frac{\partial C_A}{\partial x} = 0 \text{ and } C_A = 0;\ x = x_{critical}(t) \\ &C_A = 0 \qquad t = 0;\ x_{critical} \le x < L \end{aligned} \tag{20}$$

The zero-flux boundary condition at $x_{critical}$ is reminiscent of a boundary layer problem because the central core is nutrient-starved at short times for all reasonable values of the intra-tissue Damköhler number. Introduction of dimensionless variables for nutrient molar density, spatial position in the thinnest dimension of the sample, and time, yields;

$$\begin{aligned} &\text{Nutrient molar density; } \Psi_A = \frac{C_A}{C_{A,medium}} \\ &\text{Spatial coordinate in thinnest dimension; } \eta = \frac{x}{L} \\ &\text{Dimensionless diffusion time; } \tau = \frac{tD_{\mathrm{A,effective,intra-tissue}}}{L^2} = \frac{t}{\Theta_{Diffusion}} \end{aligned} \tag{21}$$

where $\Theta_{Diffusion}$ represents a characteristic time constant for intra-tissue diffusion. This allows one to re-express the modified diffusion equation and its boundary conditions in dimensionless form;

$$\begin{aligned} &\frac{\partial \Psi_A}{\partial \tau} = \frac{\partial^2 \Psi_A}{\partial \eta^2} - \Lambda_A^2 \Psi_A^n \\ &\Psi_A = 1;\ \eta = 1;\ \tau > 0 \\ &\frac{\partial \Psi_A}{\partial \eta} = 0 \text{ and } \Psi_A = 0;\ \eta = \eta_{critical}(\tau) \\ &\Psi_A = 0;\ \tau = 0;\ \eta_{critical} \le \eta < 1 \end{aligned} \tag{22}$$

A *combination-of-variables* solution to Eq. (22) via the penetration theory is provided in reference [11], and perturbation analysis of mass transfer with zeroth-order chemical reaction is described in reference [12]. There are very few literature references that invoke the von Kármán–Pohlhausen *profile* method and solve the modified diffusion equation with chemical reaction to predict transient mass transfer boundary layer thicknesses (i.e., 4 matches in Web of Science™ to *diffusion, reaction, von Kármán*).

6. Analytical solution of the modified diffusion equation via the von Kármán–Pohlhausen integral method of boundary layer analysis

6.1. Zeroth-order rates of nutrient consumption

The transient reaction–diffusion equation, Eq. (22), was written for zeroth-order nutrient consumption (i.e., $n=0$);

$$\begin{aligned}&\frac{\partial\Psi_A}{\partial\tau}=\frac{\partial^2\Psi_A}{\partial\eta^2}-\Lambda_A^2\\&\Psi_A=1;\eta=1;\tau>0\\&\frac{\partial\Psi_A}{\partial\eta}=0\text{ and }\Psi_A\Rightarrow 0;\eta=\eta_{critical}(\tau)\\&\Psi_A=0;\tau=0;\eta_{critical}\le\eta<1\end{aligned}\tag{23}$$

and solved for $\Psi_A(\varphi)$ and $\eta_{critical}(\tau;\Lambda_A)$ by postulating a quadratic function of the combined variable φ according to the von Kármán–Pohlhausen profile method of boundary layer analysis;

$$\begin{aligned}&\Psi_A(\tau,\eta)=\Psi_A(\varphi)=\beta+\gamma\varphi+\varepsilon\varphi^2\\&\varphi=\frac{1-\eta}{1-\eta_{critical}(\tau,\Lambda_A)}\end{aligned}\tag{24}$$

The proposed quadratic function for dimensionless molar density Ψ_A in Eq. (24) is consistent with the steady state profile, given by Eqs. (9) and (13), for all values of the intra-tissue Damköhler number in rectangular tissue. Boundary conditions at $\eta=1$ [i.e., $\Psi_A(\varphi=0)=1$] and $\eta=\eta_{critical}$ [i.e., $\{\partial\Psi_A/\partial\eta\}_{\varphi=1}=\Psi_A(\varphi=1)=0$] yield numerical values for the constants β, γ, and ε. Hence;

$$\begin{aligned}&\Psi_A(\varphi=0)=\beta=1\\&\Psi_A(\varphi=1)=\beta+\gamma+\varepsilon=0\\&\left\{\frac{\partial\Psi_A}{\partial\eta}\right\}_{\eta=\eta_{critical}}=\frac{-1}{1-\eta_{critical}(\tau,\Lambda_A)}\left\{\frac{\partial\Psi_A}{\partial\varphi}\right\}_{\varphi=1}=\frac{-\gamma-2\varepsilon}{1-\eta_{critical}(\tau,\Lambda_A)}=0\end{aligned}\tag{25}$$

with $\beta=1$, $\gamma=-2$, $\varepsilon=1$. If $\Psi_A\Rightarrow 0$ with zero slope at $\varphi=1$, then the initial condition is satisfied as $\varphi\Rightarrow\infty$. Upon substitution of the postulated profile for $\Psi_A(\varphi)$ via Eq. (24) into Eq. (23), multiplication by $1-\eta_{critical}$, and integration with respect to η from $\eta_{critical}$ to 1 at constant τ, or, preferably, integration with respect to φ from 0 to 1, it is possible to obtain a first-order ordinary differential equation (ODE) for $\eta_{critical}(\tau,\Lambda_A)$ that represents conservation of species mass over the thickness of the boundary layer. This is illustrated in Eq. (26).

$$\begin{aligned}&\left\{\frac{\partial\Psi_A}{\partial\tau}\right\}_\eta=\frac{d\Psi_A}{d\varphi}\left\{\frac{\partial\varphi}{\partial\eta_{critical}}\right\}_\eta\frac{d\eta_{critical}}{d\tau}=\frac{\varphi}{1-\eta_{critical}}\{\gamma+2\varepsilon\varphi\}\frac{d\eta_{critical}}{d\tau}\\&\left\{\frac{\partial^2\Psi_A}{\partial\eta^2}\right\}_\tau=\frac{1}{\{1-\eta_{critical}\}^2}\frac{d^2\Psi_A}{d\varphi^2}=\frac{2\varepsilon}{\{1-\eta_{critical}\}^2}\\&\frac{d\eta_{critical}}{d\tau}\int_0^1\varphi\{\gamma+2\varepsilon\varphi\}d\varphi=\left\{\frac{1}{2}\gamma+\frac{2}{3}\varepsilon\right\}\frac{d\eta_{critical}}{d\tau}=-\frac{1}{3}\frac{d\eta_{critical}}{d\tau}\\&\qquad=\frac{2}{1-\eta_{critical}}-\Lambda_A^2\{1-\eta_{critical}\}\end{aligned}\tag{26}$$

The differential equation for $\eta_{critical}(\tau,\Lambda_A)$ in Eq. (26) reduces to Eq. (11) at steady state when $\eta_{critical}$ is independent of dimensionless diffusion time τ. Eq. (26) is solved analytically for $\eta_{critical}(\tau,\Lambda_A)$, subject to the initial condition $\eta_{critical}(\tau=0)=1$;

$$\tau=\frac{1}{3}\int_{\eta_{critical}}^{1}\frac{(1-y)dy}{2-\Lambda_A^2(1-y)^2}=\frac{1}{6\Lambda_A^2}\ln\left\{\frac{2}{2-\Lambda_A^2[1-\eta_{critical}]^2}\right\}$$

$$\{\delta_{MTBLT}(\tau;\Lambda_A)\}_{Zeroth-order}=1-\eta_{critical}(\tau;\Lambda_A)=\frac{\sqrt{2}}{\Lambda_A}\sqrt{1-\exp\{-6\Lambda_A^2\tau\}}\tag{27}$$

Time-dependent growth of the dimensionless mass transfer boundary layer $\delta_{MTBLT}(\tau,\Lambda_A)$, measured inward from the external tissue surface is predicted from the modified diffusion equation, Eq. (23). The region defined by, $1-\delta_{MTBLT}\le\eta\le 1$, contains the ingredients required for cell proliferation within regenerative matrices and biocatalytic sensors. Steady state conditions are achieved at shorter dimensionless diffusion times τ when the intra-tissue Damköhler number is larger. At sub-critical intra-tissue Damköhler numbers [i.e., $\Lambda_A<\sqrt{(2)}$], $\delta_{MTBLT}(\tau\Rightarrow\infty)\Rightarrow 1$ when steady state conditions are achieved.

6.2. First-order rates of nutrient consumption

Biosensors are miniaturized analytical devices that determine the concentration of substances and other parameters of biological interest. The biologically responsive event could be a whole cell metabolism, protein–ligand binding, or antibody–antigen reactions. Successful biosensors possess the following features: (i) the biocatalyst is highly specific, (ii) reactions are independent of stirring, pH, ionic strength, temperature, and inhibitors, and (iii) the probe is biocompatible, with no toxic or antigenic effects. Response of *third-generation* sensors occurs when biocatalytic membranes convert substrates to products, and a transducer detects physicochemical changes that accompany the reaction. When reactions are diffusion-limited at large Damköhler numbers, apparent first-order kinetics are measured. Eq. (22) was written for transient diffusion and first-order nutrient consumption (i.e., $n=1$), with zero flux and zero molar density at the leading edge of the inward growing nutrient boundary layer;

$$\begin{aligned}&\frac{\partial\Psi_A}{\partial\tau}=\frac{\partial^2\Psi_A}{\partial\eta^2}-\Lambda_A^2\Psi_A\\&\Psi_A=1;\eta=1;\tau>0\\&\frac{\partial\Psi_A}{\partial\eta}=0\text{ and }\Psi_A\Rightarrow 0;\eta=1-\delta_{MTBLT}(\tau)\\&\Psi_A=0;\tau=0;1-\delta_{MTBLT}(\tau)\le\eta<1\end{aligned}\tag{28}$$

Analogous to zeroth-order kinetics in the previous section, Eq. (28) was solved for $\Psi_A(\varphi)$ and $\delta_{MTBLT}(\tau;\Lambda_A)$ by postulating a quadratic function of the combined variable φ;

$$\begin{aligned}&\Psi_A(\tau,\eta)=\Psi_A(\varphi)=\beta+\gamma\varphi+\varepsilon\varphi^2\\&\varphi=\frac{1-\eta}{\delta_{MTBLT}(\tau,\Lambda_A)}\end{aligned}\tag{29}$$

Boundary conditions at $\eta=1-\delta_{MTBLT}$ and $\eta=1$ yield numerical values for the constants β, γ, and ε that are the same as those in Eq. (25). Once again, von Kármán–Pohlhausen analysis yields a first-order ordinary differential equation for $\delta_{MTBLT}(\tau,\Lambda_A)$ that is solved analytically and compared with the dimensionless mass transfer

boundary layer thickness for zeroth-order nutrient consumption [see Eq. (27)];

$$-\frac{d\delta_{MTBLT}}{d\tau}\int_{\varphi=0}^{\varphi=1}\{\varphi(\gamma+2\varepsilon\varphi)\}d\varphi=\frac{2\varepsilon}{\delta_{MTBLT}}-\Lambda_A^2\delta_{MTBLT}\int_{\varphi=0}^{\varphi=1}\left\{\beta+\gamma\varphi+\varepsilon\varphi^2\right\}d\varphi$$
$$\frac{d\delta_{MTBLT}}{d\tau}=\frac{6}{\delta_{MTBLT}}-\Lambda_A^2\delta_{MTBLT} \tag{31}$$

The initial condition is $\delta_{MTBLT}=0$ when $\tau=0$. Hence;

$$\tau=\int_0^{\delta_{MTBLT}}\frac{ydy}{6-\Lambda_A^2y^2}=\frac{1}{2\Lambda_A^2}\ln\left\{\frac{6}{6-\Lambda_A^2\delta_{MTBLT}^2}\right\} \tag{32}$$
$$\{\delta_{MTBLT}(\tau;\Lambda_A)\}_{1^{st}-order}=\frac{\sqrt{6}}{\Lambda_A}\sqrt{1-\exp\{-2\Lambda_A^2\tau\}}$$

Eqs. (27) and (32) reveal that transient and steady state mass transfer boundary layer thicknesses are larger for first-order rates of consumption, relative to zeroth-order rates of consumption. Steady state conditions are achieved at shorter dimensionless diffusion times τ for zeroth-order kinetics, relative to first-order kinetics. Generalized von Kármán–Pohlhausen analysis of the unsteady state reaction–diffusion equation for simple nth-order rates of consumption in regenerative tissue and biocatalytic sensors with rectangular symmetry yields the following expression for the dimensionless mass transfer boundary layer thickness;

$$\{\delta_{MTBLT}(\tau;\Lambda_A)\}_{n^{th}-order}=\frac{a_1(n;\kappa)}{\Lambda_A}\sqrt{1-\exp\{-a_2(n;\kappa)\Lambda_A^2\tau\}} \tag{33}$$
$$\kappa=\int_{\varphi=0}^{\varphi=1}\left\{\beta+\gamma\varphi+\varepsilon\varphi^2\right\}^n d\varphi\overset{\beta=\varepsilon=1}{\underset{\gamma=-2}{\Rightarrow}}\left\{\begin{matrix}1;n=0\\ \frac{1}{3};n=1\\ \frac{1}{5};n=2\end{matrix}\right\};$$
$$a_1(n;\kappa)=\sqrt{\frac{6}{3\kappa}};\ a_2(n;\kappa)=6\kappa$$

where the coefficients, a_1 and a_2, depend on reaction order n and the parameter κ, as summarized in Eq. (33) and Table 2, and $\delta_{MTBLT}(\tau\Rightarrow\infty)\Rightarrow 1$ when $\Lambda_A<a_1(n)$.

7. von Kármán–Pohlhausen analysis of unsteady state radial diffusion and simple nth-order consumption in biomaterials with cylindrical and spherical symmetry

The transient reaction–diffusion equation, Eq. (22), was written for nth-order nutrient consumption in curvilinear coordinates with a "curvature correction" given by Eq. (15);

$$\frac{\partial\Psi_A}{\partial\tau}=\frac{1}{\eta^\alpha}\frac{\partial}{\partial\eta}\left\{\eta^\alpha\frac{\partial\Psi_A}{\partial\eta}\right\}-\Lambda_A^2\Psi_A^n=\frac{\partial^2\Psi_A}{\partial\eta^2}+\frac{\alpha}{\eta}\frac{\partial\Psi_A}{\partial\eta}-\Lambda_A^2\Psi_A^n$$
$$\Psi_A=1;\eta=1;\tau>0$$
$$\frac{\partial\Psi_A}{\partial\eta}=0\text{ and }\Psi_A\Rightarrow 0;\eta=\eta_{critical}(\tau) \tag{34}$$
$$\Psi_A=0;\tau=0;\eta_{critical}\le\eta<1$$

Table 2
Effect of reaction order n for simple nth-order rates of nutrient consumption on the coefficients a_1 and a_2 in the generalized prediction for the dimensionless mass transfer boundary layer thickness via Eq. (33), according to the von Kármán–Pohlhausen integral method of boundary layer analysis in biomaterials with rectangular symmetry.

Reaction order, n	κ	a_1	a_2
0	1	√(2)	6
1	1/3	√(6)	2
2	1/5	√(10)	6/5

Nutrient molar density $\Psi_A(\varphi)$ was postulated as a quadratic function of the combined variable φ according to Eq. (24), which is approximately consistent with the distorted quadratic steady state profiles given by Eq. (16) when $n=0$. When the rate of nutrient consumption follows simple nth-order kinetics, dimensionless mass transfer boundary layer thicknesses in regenerative tissue and biocatalytic sensors with rectangular (i.e., $\alpha=0$), cylindrical (i.e., $\alpha=1$), or spherical (i.e., $\alpha=2$) symmetry are governed by the following equations for $\eta_{critical}(\tau;\Lambda_A)$, where $\delta_{MTBLT}(\tau;\Lambda_A)=1-\eta_{critical}(\tau;\Lambda_A)$;

$$-\frac{1}{3}\frac{d\eta_{critical}}{d\tau}=\frac{2}{1-\eta_{critical}}+2\alpha\int_0^1\frac{(1-\varphi)d\varphi}{1-\varphi\{1-\eta_{critical}\}}-\Lambda_A^2\{1-\eta_{critical}\}\int_{\varphi=0}^{\varphi=1}\left\{\beta+\gamma\varphi+\varepsilon\varphi^2\right\}^n d\varphi$$
$$\tau=\frac{1}{3}\int_{\eta_{critical}}^1\frac{(1-y)dy}{2-\kappa\Lambda_A^2(1-y)^2+2\alpha(1-y)\int_0^1\frac{(1-\varphi)d\varphi}{1-\varphi(1-y)}} \tag{35}$$

Eq. (35) reduces to Eqs. (26) and (27) for zeroth-order consumption in biomaterials with rectangular symmetry when $n=0$, $\kappa=1$, and the curvature correction constant $\alpha=0$. One obtains Eqs. (31) and (32) for first-order consumption in biomaterials with rectangular symmetry when $n=1$, $\kappa=1/3$, and $\alpha=0$. Due to the complexity of the integral in Eq. (35), the first-order ODE for $\eta_{critical}(\tau;\Lambda_A)$ is solved numerically to compare mass transfer boundary layer thicknesses for all three biomaterial geometries and reaction orders;

$$\frac{d\eta_{critical}}{d\tau}=3\kappa\Lambda_A^2\{1-\eta_{critical}\}-\frac{6}{1-\eta_{critical}}-6\alpha\int_0^1\frac{(1-\varphi)d\varphi}{1-\varphi\{1-\eta_{critical}\}}$$
$$\tau=0^+;\eta_{critical}=1^-$$
$$\kappa=\int_{\varphi=0}^{\varphi=1}\left\{\beta+\gamma\varphi+\varepsilon\varphi^2\right\}^n d\varphi\overset{\beta=\varepsilon=1}{\underset{\gamma=-2}{\Rightarrow}}\left\{\begin{matrix}1;n=0\\ \frac{1}{3};n=1\\ \frac{1}{5};n=2\end{matrix}\right\}\quad\alpha=\left\{\begin{matrix}0;\text{rectangles}\\ 1;\text{cylinders}\\ 2;\text{spheres}\end{matrix}\right\}$$
$$\int_0^1\frac{(1-\varphi)d\varphi}{1-\varphi\{1-\eta_{critical}\}}=\frac{\eta_{critical}\ln\eta_{critical}+\{1-\eta_{critical}\}}{\{1-\eta_{critical}\}^2} \tag{36}$$

Similar to the conclusions drawn from inspection of Eqs. (27), (32) and (33) for biomaterials with rectangular symmetry, numerical predictions in Fig. 2 for cylindrical biomaterials reveal that transient and steady state mass transfer boundary layer thicknesses increase when the exponent n is larger, for nth-order rates of consumption, but steady state conditions are achieved at shorter dimensionless diffusion times τ when n is smaller. The lowermost curve in Fig. 2 for cylindrical biomaterials with $\Lambda_A=4$ yields a *steady state* dimensionless mass transfer boundary layer thickness of 0.39 at $\tau=0.1$, which is in excellent agreement with the root of Eq. (16a) for $\eta=\eta_{critical}$ vs. Λ_A in Table 1 when radial diffusion and zeroth-order consumption in cylindrical coordinates reveal that $\delta_{MTBLT}(\tau\Rightarrow\infty)=1-\eta_{critical}=0.38$. Results in Fig. 3 reveal the effect of biomaterial geometry on the solution of Eq. (36) for simple 1st-order rates of nutrient consumption. The curvature correction for radial diffusion in cylinders and spheres, given by the last term on the right side of the ODE for $\eta_{critical}$ in Eq. (36), increases the transient and steady state boundary layer thicknesses relative to the lowermost curve in Fig. 3 for biomaterials with rectangular symmetry.

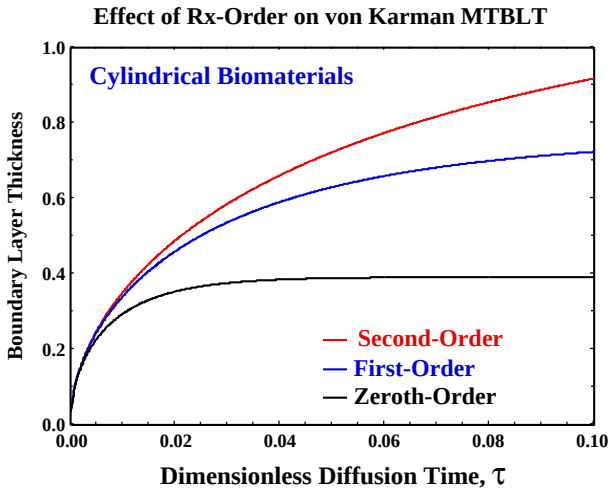

Fig. 2. Numerical solution of Eq. (36) for cylindrical biomaterials (i.e., $\alpha=1$). Time-dependent dimensionless mass transfer boundary layer thickness, measured inward from the outer surface, is illustrated for simple nth-order kinetics (i.e., $n=0,1,2$). Reaction order n increases from the lowermost curve to the uppermost curve. Dimensionless diffusion time τ on the horizontal axis is defined in Eq. (21), and the intra-tissue Damköhler number $\Lambda_A=4$ is greater than its critical value. According to the analytical solution in rectangular coordinates, given by Eq. (33), the following *initial condition* was employed; $\delta_{MTBLT}=1-\eta_{critical}=0.0346$ at $\tau=10^{-4}$ when $\Lambda_A=4$.

8. Numerical analysis of the modified diffusion equation with first-order consumption in regenerative tissue and biocatalytic sensors

Finite-difference calculus was employed to solve Eq. (22) with a zero-flux boundary condition in the central tissue core at $x=0$, for biomaterials with rectangular symmetry. The concept of $\eta_{critical}$ is not required mathematically when $n=1$ for 1st-order kinetics. Consequently, zero flux and vanishing nutrient molar density at $\eta_{critical}$ are not employed to solve the PDE for $\Psi_A(\tau,\eta)$. Comparisons in Table 3 reveal that the exact form of the boundary conditions affects the magnitude of the boundary layer thicknesses. von Kármán–Pohlhausen boundary layer calculations for 1st-order nutrient consumption in biomaterials with rectangular symmetry, according to Eq. (33) and Table 2, yield smaller values of $\delta_{MTBLT}(\tau;\Lambda_A)$ than those determined from finite-difference-based intra-tissue local molar density profiles for 1st-order nutrient consumption, illustrated in Fig. 4. Finite-difference profiles are integrated at each time step and presented as transient volume-averaged profiles in Fig. 5. Simulations in Figs. 4 and 5 satisfy a *quasi-macroscopic* version of the unsteady mass balance [4] in which diffusion only provides a contribution at the biomaterial interface with the well-mixed medium (i.e., $\eta=\pm1$), in agreement with the zero-flux boundary condition in the tissue's central core at $x=0$. Transient profiles in Fig. 4 reveal inward growth of the mass transfer boundary layer at longer dimensionless diffusion times τ. A complete summary of transient mass transfer boundary layer predictions in biomaterials with rectangular symmetry, calculated analytically via Eqs. (27) and (32), and numerically via Fig. 4, is presented in Table 3 when the rate of nutrient consumption is described by simple zeroth-order and first-order kinetics.

If biocatalytic sensors respond to a volumetric average of the diffusing species within the regenerative matrix, then transient sensor response is illustrated in Fig. 5. Steady state behavior is achieved

Table 3
Comparison of dimensionless mass transfer boundary layer thicknesses for zeroth-order and first-order rates of nutrient consumption in regenerative tissue and biocatalytic sensors with rectangular symmetry as a function of dimensionless diffusion time τ and the intra-tissue Damköhler number Λ_A.

Λ_A	τ	δ_{MTBLT}, $n=0$ von Kármán–Pohlhausen Eq. (27)	δ_{MTBLT}, $n=1$ von Kármán–Pohlhausen Eq. (32)	δ_{MTBLT}, $n=1$ finite difference Fig. 4
√(2)	0.007	0.28	0.29	0.30
√(2)	0.030	0.55	0.58	0.63
√(2)	0.050	0.67	0.74	0.81
5	0.007	0.23	0.27	0.30
5	0.030	0.28	0.43	0.58
5	0.050	0.28	0.47	0.70
10	0.007	0.14	0.21	0.28
10	0.030	0.14	0.24	0.43
10	0.050	0.14	0.25	0.45

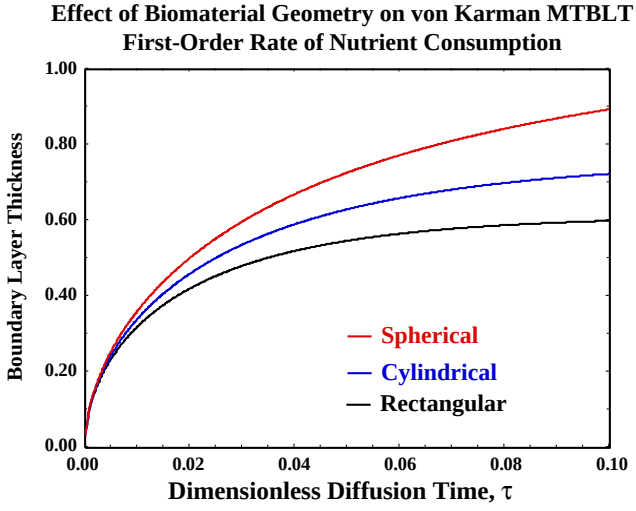

Fig. 3. Numerical solution of Eq. (36) for simple first-order nutrient consumption (i.e., $n=1$). Time-dependent dimensionless mass transfer boundary layer thickness, measured inward from the outer surface, is illustrated for biomaterials with rectangular ($\alpha=0$, lowermost curve), cylindrical ($\alpha=1$, middle curve), and spherical ($\alpha=2$, uppermost curve) symmetry. Dimensionless diffusion time τ on the horizontal axis is defined in Eq. (21), and the intra-tissue Damköhler number $\Lambda_A=4$ is greater than its critical value for all geometries. According to the analytical solution in rectangular coordinates, given by Eq. (33), the following *initial condition* was employed; $\delta_{MTBLT}=1-\eta_{critical}=0.0346$ at $\tau=10^{-4}$ when $\Lambda_A=4$.

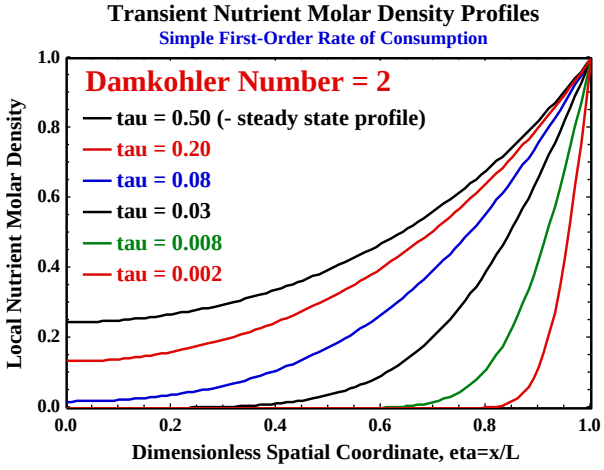

Fig. 4. Numerical analysis of dimensionless nutrient molar density vs. spatial coordinate η for one-dimensional diffusion and simple first-order consumption at various dimensionless diffusion times τ via Eq. (22). τ increases from the lowermost curve to the uppermost curve. The intra-tissue Damköhler number Λ_A is greater than its critical value for regenerative tissue and biocatalytic sensors with rectangular geometry. The thinnest spatial dimension (i.e., x) is divided equally into 101 mesh points for finite-difference calculations. The analytical molar density profile at steady state is given by [4,5,10]: $\Psi_A(\eta,\Lambda_A)=\cosh(\Lambda_A\eta)/\cosh(\Lambda_A)$, uppermost curve, which yields $\Psi_A(\eta=0,\Lambda_A)=1/\cosh(\Lambda_A)=0.266$ in the tissue's central core when $\Lambda_A=2$.

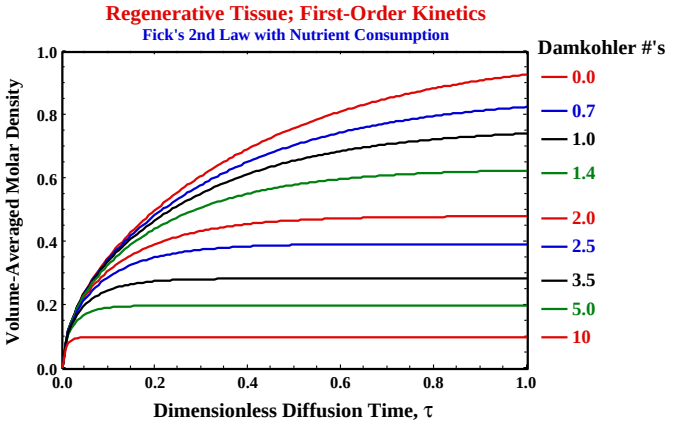

Fig. 5. Transient biomaterial-averaged dimensionless molar density vs. dimensionless diffusion time τ for one-dimensional diffusion and simple first-order consumption in regenerative tissue and biocatalytic sensors with rectangular geometry. The intra-tissue Damköhler number Λ_A increases from the uppermost curve to the lowermost curve. The thinnest spatial dimension (i.e., x) is divided equally into 101 mesh points for finite-difference calculations and numerical integration. Analytical integration of the dimensionless molar density profile at steady state (i.e., see the caption to Fig. 4) yields the effectiveness factor [4]: $\int \Psi_A(\eta,\Lambda_A)d\eta = \{\tanh(\Lambda_A)\}/\Lambda_A$.

at shorter dimensionless diffusion times τ when the intra-tissue Damköhler number is larger, as one approaches the diffusion-limited regime. Biomaterial-averaged molar density vs. diffusion time τ allows one to estimate the time required to achieve steady state conditions for regenerative tissue growth and biocatalytic sensing, based on the time constant for intra-tissue diffusion in Eq. (21), $L^2/D_{A,effective\ \text{intra-}tissue}$.

9. Conclusions

The steady state aspects of this investigation were inspired by Ref. [1], which reveals qualitative reactant molar density profiles in biomaterial matrices with rectangular symmetry. However, it is obvious that the inappropriate boundary conditions were employed when the intra-tissue Damköhler number exceeds its geometry-sensitive critical value and the required ingredients necessary for cell proliferation are not available in the tissue's central core. This contribution corrects those deficiencies for biomaterials with rectangular symmetry, and provides additional predictions for steady state radial diffusion and zeroth-order consumption in cylindrically and spherically shaped tissue. The critical intra-tissue Damköhler number (i.e., $\Lambda^2_{A,\text{critical}}$) is 2, 4, or 6 for one-dimensional diffusion and zeroth-order consumption in biomaterials with rectangular, cylindrical, or spherical symmetry, respectively, when the characteristic length L in the definition of the Damköhler number [i.e., see Eq. (2)] is (i) one-half of the tissue thickness in its thinnest dimension (rectangular symmetry), or (ii) the biomaterial radius for regenerative matrices and biosensors that conform to cylindrical or spherical geometry. It is desirable to develop regenerative tissue under steady state reaction–diffusion conditions when the intra-tissue Damköhler number is less than its critical value to guarantee that the entire porous biomaterial matrix or biocatalytic sensor is exposed to nutrients, oxygen, and growth factors. The von Kármán–Pohlhausen *profile* method of boundary layer analysis and finite-difference solution of the reaction–diffusion equation reveal time-dependent growth of the mass transfer boundary layer inward from the external tissue/nutrient–medium interface toward the central core. Transient boundary layer predictions are compared for n^{th}-order rates of consumption, with $n = 0,1,2$, in biomaterials of various geometry. The dimensionless diffusion time τ required to achieve steady state conditions for regenerative growth and biocatalytic sensing ranges from $0.05 < \tau < 2$, dependent upon the exponent n, for n^{th}-order rates of consumption, and the intra-tissue Damköhler number, where τ is defined in Eq. (21).

Nomenclature

a_1, a_2	coefficients in the generalized expression for the mass transfer boundary layer thickness, according to the von Kármán–Pohlhausen integral method, see Eq. (33)
C_A	molar density of nutrients, oxygen, or growth factor
$C_{A,medium}$	reactant molar densities in the liquid-phase medium that surrounds the tissue
$C_{A,Surface}$	reactant molar density on the external biomaterial surface
$D_{A,effective}$	intra-tissue diffusion coefficient for species A
E	effectiveness factor (dimensionless), equivalent to the volume fraction of biomaterial that contains the necessary ingredients for cell proliferation, when the kinetics are zeroth-order
$k_{Rx,n}$	kinetic rate constant for n^{th}-order pseudo-homogeneous rate of consumption; $\{\text{volume/mol}\}^{n-1}$/time
L	characteristic length scale for the intra-tissue Damköhler number [see Eq. (2)]; one-half of the thickness of rectangular tissue in the thinnest dimension, or the radius R of cylindrical and spherical biomaterials
n	order of the irreversible rate of reactant consumption
R^*	dimensionless rate of reactant consumption, for simple n^{th}-order kinetics, see Eq. (3)
$S_{external}$	external surface area of a tissue-engineered biomaterial
t	independent variable for transient response, time
T	absolute temperature
$T_{Surface}$	absolute temperature on the external biomaterial surface
V_{tissue}	bulk tissue volume
x	spatial coordinate measured in the thinnest dimension of rectangular tissue, or the radial direction in cylindrical and spherical biomaterials
$x_{critical}$	critical value of the spatial coordinate, below which reactants do not penetrate the central core of the tissue
y	integration variable in Eqs. (27), (32), (35)

Greek symbols

α	curvature correction constant for radial diffusion in curvilinear coordinates
β,γ,ε	coefficients in the quadratic function for dimensionless molar density Ψ_A, see Eqs. (24) and (29)
δ_{MTBLT}	time-dependent dimensionless mass transfer boundary layer thickness, measured inward from the external biomaterial surface, $= 1 - \eta_{critical}$
∇	gradient operator
φ	combined variable in the von Kármán–Pohlhausen quadratic molar density profile, see Eqs. (24) and (29)
κ	coefficient defined in Eqs. (33) and (36) that characterizes a boundary layer average of the rate of nutrient consumption in the von Kármán–Pohlhausen method of analysis
Λ_A	intra-tissue Damköhler number, which represents an order-of-magnitude estimate of the consumption rate with respect to the rate of species-specific diffusion toward the central tissue core, see Eq. (2)
$\Lambda_{A,critical}$	critical value of the intra-tissue Damköhler number, above which the central tissue core is starved of necessary ingredients required for cell proliferation
η	dimensionless spatial coordinate in the thinnest dimension of tissue with rectangular symmetry (i.e., $\eta = x/L$), or the radial direction r in cylinders and spheres (i.e., $\eta = r/R$); Eq. (21)
$\eta_{critical}$	critical value of the dimensionless spatial coordinate, below which reactants do not penetrate into the tissue's central core when $\Lambda_A > \Lambda_{A,critical}$
Ψ_A	dimensionless molar density of reactant A (nutrients, oxygen, or growth factors), defined in Eq. (21)
$\Theta_{Diffusion}$	characteristic time constant for intra-tissue diffusion; $L^2/D_{A,effective,\ \text{intra-}tissue}$
τ	dimensionless independent time variable, defined in Eq. (21)

Acknowledgements

LA Belfiore gratefully acknowledges the Provincia Autonoma di Trento for research support during his extended sabbatical at the University of Trento. Professor Matt Kipper in the Department of Chemical and Biological Engineering at Colorado State University has been a source of inspirational support throughout all of these tissue-based bioreactor simulations. Michael Floren, a PhD student in the Department of Materials Engineering and Industrial Technologies at the University of Trento, is acknowledged for helpful discussions about cell proliferation in porous biomaterials, and sending LA Belfiore the 2006 publication from *Nature Reviews in Molecular and Cell Biology* (i.e., Ref. [1]).

References

[1] L.G. Griffith, M.A. Swartz, Capturing complex 3D tissue physiology in vitro, Nature Reviews in Molecular and Cell Biology 7 (3) (March 2006) 211–224.
[2] R. Baronas, F. Ivanauskas, J. Kulys, Mathematical Modeling of Biosensors: An Introduction for Chemists and Mathematicians, Springer, Heidelberg, 2010.
[3] B.A. Grzybowski, Chemistry in Motion: Reaction–Diffusion Systems for Micro- and Nano-technology, Wiley, Hoboken, NJ, 2009.
[4] L.A. Belfiore, Transport Phenomena for Chemical Reactor Design, Wiley, Hoboken, NJ, 2003, Chaps. 16, 20, 23.
[5] G.A. Truskey, F. Yuan, D.F. Katz, Transport Phenomena in Biological Systems, 2nd ed, Prentice Hall, Upper Saddle River, NJ, 2009, Chap. 10.
[6] R. Peerani, K. Onishi, A. Mahdavi, E. Kumacheva, P.W. Zandstra, Manipulation of signaling thresholds in "engineered stem cell niches" identifies design criteria for pluripotent stem cell screens, PLoS ONE 4 (7) (July 2009) e6438, doi:10.1371/journal.pone.0006438.
[7] Y. Zeng, T.S. Lee, P. Yu, H.T. Low, Numerical simulation of mass transport in microchannel bioreactors with cell micro-patterning, Journal of Biomechanical Engineering: Transactions of ASME 130 (3) (June 2008), article #031018.
[8] M.E.G. Lyons, Transport and kinetics at carbon nanotube-redox enzyme composite modified electrode biosensors: redox enzymes dispersed in nanotube meshes of finite thickness, International Journal of Electrochemical Science 4 (2009) 1196–1236.
[9] L.A. Belfiore, W. Bonani, M. Leoni, C.J. Belfiore, Pressure-sensitive nutrient consumption via dynamic normal stress in rotational bioreactors, Biophysical Chemistry 140 (1–3) (March 2009) 99–107.
[10] R.B. Bird, W.E. Stewart, E.N. Lightfoot, Transport Phenomena, 2nd ed, Wiley, Hoboken, NJ, 2002, Chap. 18.
[11] Y.T. Shah, V.G. Pangarka, M.M. Sharma, Criteria for supersaturation in gas–liquid reactions involving a volatile product, Chemical Engineering Science 29 (7) (1974) 1601–1612.
[12] J.P. Lopes, S.S.S. Cardoso, A.E. Rodrigues, Convection, diffusion, and exothermic zeroth-order reaction in a porous catalyst slab—scaling and perturbation analysis, AIChE Journal 55 (10) (2009) 2686–2699.